Acta Manilana 73 (2025), 52-66

ISSN: 0065-1370

Acta Manilana

journal homepage: https://actamanilana.ust.edu.ph/

PTP1B Inhibitors of Marine Sponge-Derived Secondary Metabolites from *Dysidea*

Gabriel Anthony J. Lasam[1], Margaret Nicole C. Aguila[1], Ayra Joan A. De Jesus[1], Gabriela Grace M. Guzman[1], Vincent Jego M. Jontillano[1], Joe Anthony H. Manzano[1,2,3]*, John Donnie A. Ramos[1,3], & Irvin B. Rondolo[4]*

[1]Department of Biological Sciences, College of Science, University of Santo Tomas, España Blvd., Manila 1015, Philippines
[2]UST Laboratories for Vaccine Sciences, Molecular Biology, and Biotechnology, University of Santo Tomas, España Blvd., Manila 1015, Philippines
[3]Allergy and Immunology Laboratory, Research Center for Natural and Applied Sciences, University of Santo Tomas, España Blvd., Manila 1015, Philippines
[4]Department of Biology, School of Science and Engineering, Ateneo de Manila University. Katipunan Avenue, Loyola Heights, Quezon City, 1108 Philippines

Graphical Abstract

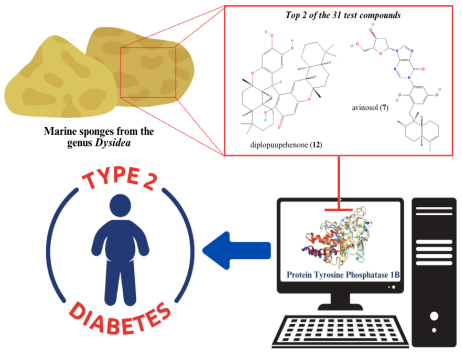

Abstract

Diabetes is a chronic metabolic disease with high morbidity and mortality due to its complications. Recently, there has been growing interest in identifying new bioactive compounds, including marine-derived secondary metabolites, for potential antidiabetic activities. This study focuses on secondary metabolites from marine sponges from the genus *Dysidea* that show strong inhibition of protein tyrosine phosphatase 1B (PTP1B), a key target in antidiabetic therapy. Thirteen out of the thirty-one compounds were identified to have promising in silico potentials vs PTP1B: avarol (**1**), avarone (**2**), furodysin (**3**), nakafuran 8 (**4**), haterumadysin A (**5**), pyrodysinoic acid (**6**), avinosol (**7**), puupehenone (**8**), α-santonin (**9**), 4'-methylaminoavarone (**10**), 3'-methylaminoavarone (**11**), diplopuupehenone (**12**), and dysideanin B (**13**). Among these, **12** showed the highest binding energy (-7.9 kcal/mol). All 13 compounds were predicted to have a favorable drug-likeness and pharmacokinetic profile, except compounds **7** and **12**. These computational findings suggest that secondary metabolites from the marine sponge *Dysidea*, particularly those with strong binding affinities and good drug-like properties, could serve as promising candidates for developing new generation anti-diabetic drugs and further *in vitro* confirmatory tests.

Keywords: diabetes, *in silico*, marine sponges, secondary metabolites, *Dysidea*, molecular docking

Corresponding authors: jhmanzano@ust.edu.ph; irondolo@ateneo.edu
DOI: https://doi.org/10.53603/actamanil.73.2025.mbrg4957

Date Received: 11 June 2025
Date Revised: 14 July 2025
Date Accepted: 14 July 2025

Introduction

Diabetes remains a major global health concern, with type 2 diabetes (T2D) accounting for over 95% of all cases worldwide [1]. In the Philippines alone, around 4.2 million cases of diabetes were reported and an estimated 2.3 million Filipinos were still undiagnosed in 2021 [2]. T2D is characterized by chronic insulin resistance and hyperglycemia, which can lead to severe complications affecting vital organs. Although current treatments such as insulin, biguanides, α-glucosidase inhibitors, and thiazolidinediones are available, their use is often limited by side effects like hypoglycemia and weight gain [3-4] highlighting the need for alternative therapies and potentially novel targets.

Protein Tyrosine Phosphatase 1B (PTP1B), a cytosolic enzyme in the PTP superfamily, is a promising therapeutic target due to its role in negatively regulating insulin and leptin signaling [5-6]. Increased PTP1B activity is associated with metabolic disorders, including diabetes, obesity, cardiovascular diseases, and Alzheimer's disease. Its conserved catalytic motif ($C(X)_5R$) makes it a key modulator in signal transduction [7-8]. Studies have shown that PTP1B knockout models exhibit protection against obesity and diabetes, further validating it as a drug target [9-10].

Natural products continue to be a valuable source of therapeutic agents. Marine organisms, particularly sponges, have been shown to contain bioactive compounds with anti-diabetic potential. For example, bromophenols from *Rhodomela confervoides* inhibit both PTP1B and α-glucosidase [11], while dysidine from *Dysidea* sp. shows strong PTP1B inhibition and promising therapeutic potential [12]. Other species in the *Dysidea* genus, such as *D. avara*, *D. granulosa*, and *D. herbacea*, produce diverse compounds like sesquiterpenoids and polybrominated diphenyl ethers with notable bioactivities [13-14].

With drug discovery becoming increasingly resource-intensive, *in silico* approaches now offer efficient alternatives for early-stage screening. Structure-Based Drug Design (SBDD) and Ligand-Based Drug Design (LBDD) are widely used to identify and optimize lead compounds [15-17]. These tools have been successfully applied across various disease areas, including infectious [18-19], tumorigenic [20], and neurodegenerative diseases and disorders [21]. Several studies have also utilized *in silico* methodologies to target enzymes implicated in diabetes [22-23]. In this study, we employed *in silico* screening to evaluate marine sponge-derived secondary metabolites from *Dysidea* for their potential as PTP1B inhibitors in T2D treatment.

Materials and methods

Screening of metabolites from the genus Dysidea and ligand preparation. A total of 31 secondary metabolites previously reported to be isolated from the genus *Dysidea* were selected. The following are the ligands used in the study: dysidine, dysidotronic acid, dysidenone A, furodysin, bolinaquinone, 7-deacetoxyolepupuane, avinosol, dendrolasin, puupehenone, dysidamide D, dicynone, diplopuupehenone, dysithiazolamide, dysideanin A, and dysideanin B (isolated from *Dysidea* sp.); avarol, avarone, α-santonin, 4'- methylaminoavarone, and 3'-methylaminoavarone (isolated from *Dysidea avara*);

nakafuran 8, nakafuran 9, dehydroherbadysidolide, and dysideasterol F (isolated from *Dysidea fragilis*); haterumadysin A, B, and D (isolated from *Dysidea cholera*); arenarol (isolated from *Dysidea arenaria*); pyrodysinoic acid (isolated from *Dysidea robusta*); and isodysidenin (isolated from *Dysidea herbacea*) [24-30]. The marine secondary metabolites identified and screened from the genus *Dysidea* were acquired in PubChem (https://pubchem.ncbi.nlm.nih.gov/) and formatted in SMILES notation [31]. The prepared ligands were optimized and converted into SYBYL mol2 files and were added to the UCSF Chimera 1.15 platform [32].

Target protein preparation. The three-dimensional structure of protein tyrosine phosphatase 1B (PDB ID: 1T49) was acquired from the Protein Data Bank utilizing UCSF Chimera 1.15 platform [32]. Non-standard residues and water molecules were removed, and protein minimization was accomplished using the steepest descent method with a total of 100 steps, along with the conjugate gradient method. Charges were assigned using Amber's Antechamber computation, applying Gasteiger charge mode as reported in previous protocols [33].

Molecular docking analysis and visualization. The prepared ligands in SYBYL mol2 format were added into UCSF Chimera [32] with the prepared minimized protein. The molecules were prepared using dock prep with default configurations, and charges were assigned using Amber's Antechamber computation, also utilizing Gasteiger charge mode. Docking was initiated using Autodock Vina 1.2.0 [34], and molecules were exported as "pdbqt" files. Docking simulations were performed with a grid box size of 22.5 Å x 22.5 Å x 22.5 Å and coordinates x = 55.74, y = 33.41, and z = 24.47 for the location of the allosteric site using PTP1B (1T49). Visualization of the diagrams was carried out using BIOVIA Discovery Studio. Inhibitors with the most potential, having binding energies of -7.0 kcal/mol and below, were considered accepted values for the molecular docking results [35]. Among the 31 secondary metabolites, 13 were selected based on the acceptable score.

Pharmacokinetic and drug-likeness profiling. The drug-likeness based on Lipinski's rules of five (LRo5) was predicted using SWISSADME (http://www.swissadme.ch/index.php). The following properties were recorded: molecular weight, number of H-bond acceptors, number of H-bond donors, lipophilicity, and number of violations based on LRo5. The BOILED-Egg (Brain Or IntestinaL EstimateD permeation) method was also generated to predict pharmacokinetic profiles of the compounds. The BOILED-Egg model is a computational tool used to predict passive gastrointestinal absorption and brain penetration based on the lipophilicity (WLOGP) and polarity (TPSA) of molecules. Compounds falling within the white region of the model are predicted to be well-absorbed in the gastrointestinal tract, while those in the yellow (yolk) region are likely to cross the blood-brain barrier [36].

Results

Molecular docking. Thirty-one selected secondary metabolites from the genus *Dysidea* were molecularly docked onto the allosteric site of protein tyrosine phosphatase 1B (PDB ID:1T49) (Supplementary Table S1). The top 13 compounds that crossed the -7.0 kcal/mol threshold are shown in Table 1 and Figure 1. Five of the thirteen compounds exhibited hydrogen bonding along with other interactions.

Among the screened compounds, diplopuupehenone (**12**) exhibited the most favorable binding energy of -7.9 kcal/mol. Its catechol group was involved in hydrogen bonding with ALA189 and pi-alkyl interactions with LEU192. However, an unfavorable acceptor–acceptor interaction was noted with GLU276. Following closely, avinosol (**7**) displayed a binding energy of -7.8 kcal/mol, where its alcohol moieties, attached to an oxolane ring, formed hydrogen bonds with ARG254, TYR20, and ASP48. Notably, a salt bridge was also formed between its purine structure and residues ASP48 and ARG24.

The remaining compounds exhibited binding energies ranging from -7.6 to -7.0 kcal/mol, suggesting their potential as PTP1B inhibitors. Three compounds, namely furodysin (**3**), pyrodysinoic acid (**6**), and 3'-methylaminoavarone (**11**), recorded binding energies of -7.6 kcal/mol. Compound **3** did not form hydrogen bonds but exhibited several pi-alkyl interactions between its aliphatic hydrocarbon chains and residues PHE196 and PHE280. LEU192 and PHE280 were involved in interactions with their ethyl moieties. Compound **6** engaged in multiple hydrogen bonds via its oxygen moieties with GLN262, GLN266, ARG221, and TRP179. It also demonstrated pi-alkyl interactions between its first cyclic hydrocarbon and residues TYR46, ALA217, and VAL49. Compound **11** formed hydrogen bonds via its oxygen and hydrogen groups with ASN193 and ALA189, respectively. Pi-pi stacking interactions were observed between its cyclohexadiene group and PHE196 and PHE280, along with pi-alkyl interactions involving ethyl moieties and both residues.

Four other compounds, namely avarol (**1**), avarone (**2**), α-santonin (**9**), and 4'-methylaminoavarone (**10**), showed binding energies of -7.4 kcal/mol. Compound **1** did not exhibit hydrogen bonding but showed several pi-pi T-shaped interactions via its catechol group with PHE280, LEU12, and PHE16. Compound **2** formed a hydrogen bond through its second cyclohexenone moiety with ASN193, and pi-pi stacked interactions were noted with PHE280, LEU192, and PHE196. Additional pi-alkyl interactions were seen with the same residues. Compound **9** established a hydrogen bond through its ether and oxygen moieties with ASN193 and LYS197, respectively. Pi-alkyl interactions were also indicated with its cyclohexane moiety participating in a bond with PHE 280 and PHE196, while its methyl moieties also bound to residues LEU192, PHE196, and PHE280. Lastly, the cyclohexadiene moiety of compound **10** formed a hydrogen bond with ASN193. Pi-pi stacked interactions were noted between its cyclohexene group and residues LEU192 and PHE280. Pi-alkyl interactions were also observed between the cyclohexane and ethyl moieties and PHE196.

Table 1. Thirteen metabolites from the genus *Dysidea* with high affinity to Protein Phosphatase 1B (PTP1B) and their interactions with the residues at the allosteric binding site.

Compound	Binding energy values (kcal/mol)	Hydrogen bond	Other Interactions (pi-sigma, pi-stacked)
Avarol (**1**)	-7.4	None	PHE 280, LEU 192, PHE 196
Avarone (**2**)	-7.4	ASN193	PHE 280, LEU 192, PHE 196
Furodysin (**3**)	-7.6	None	PHE 280, LEU 192, PHE 196
Nakafuran-8 (**4**)	-7.1	None	PHE 280, LEU 192, PHE 196, ALA 189
Haterumadysin A (**5**)	-7.3	None	PHE 280, ILE 281, PHE 196
Pyrodysinoic acid (**6**)	-7.6	GLN 266, GLN 262, ARG 221, TRP 179	TYR 46, ALA 217, VAL 49
Avinosol (**7**)	-7.8	ARG 254, TYR 20, ASP 48	CYS 215, LYS 120, ASP 48, ARG 24
Puupehenone (**8**)	-7.0	GLN 266	ARG 221, SER 216
α-Santonin (**9**)	-7.4	ASN 193, LYS 197	PHE 280, LEU 192, PHE 196
4'-Methylaminoavarone (**10**)	-7.4	ASN 193	PHE 280, PHE 196
3'-Methylaminoavarone (**11**)	-7.6	ASN 193, ALA 189	PHE 280, PHE 196
Diplopuupehenone (**12**)	-7.9	ALA 189	PHE 280, LEU 192
Dysideanin B (**13**)	-7.0	GLU 276	PHE 280, LEU 192, PHE 196, ALA 189

The last set of compounds, which are nakafuran 8 (**4**) and haterumadysin A (**5**), exhibited binding energy values of -7.1 and -7.3 kcal/mol, respectively. The lowest binding affinity for the experiment exhibited -7 kcal/mol for both puupehenone (**8**) and dysideanin B (**13**). Compound **4** exhibited only pi-alkyl interactions between its cyclohexene moiety and residues PHE196, PHE280, and LEU192. Compound **5** did not present any hydrogen bonding and only pi-alkyl interactions with PHE280, ILE281, and PHE196. Compound **8** exhibited hydrogen bonding with GLN266 and salt bridge interactions with ARG221. Lastly, **13** exhibited carbon-hydrogen bonds between their hydrogen moieties and GLU276. Pi-pi stacked interactions were observed in the phenol, pyrrole, and hexadiene moieties of **13**, which interacted with LEU192 and PHE280. Pi-alkyl interactions were also noted in the hexadiene and phenol moieties, which interacted with PHE196 and ALA189, respectively.

Drug-likeness parameters and BOILED-Egg pharmacokinetic predictions. To predict the drug-likeness *in silico* of the top 13 compounds based on the Lipinski rule of five, they were subjected to SWISSADME analysis. All compounds except compound **12** exhibited favorable drug likeness (Table 2). Meanwhile, based on the BOILED-Egg model, all compounds except **7** demonstrated favorable pharmacokinetic profiles, with predicted passive gastrointestinal absorption and potential blood-brain barrier penetration. These results support their drug-likeness and bioavailability, reinforcing their viability as lead compounds for further development against PTP1B (Figure 4).

Table 2. Drug-likeness of top *Dysidea* compounds according to Lipinski's rule of five.

Compound	MW < 500 g/mol	#H-bond acceptors <10	#H-bond donors <5	Lipophilicity MLogP<4.15	Lipinski violations	Drug-likeness
Avarol (**1**)	314.46	2	2	4.39	1	Yes
Avarone (**2**)	312.45	2	2	3.77	0	Yes
Furodysin (**3**)	216.32	1	0	3.42	0	Yes
Nakafuran (**4**)	216.32	1	0	3.42	0	Yes
Haterumadysin A (**5**)	274.35	3	0	3.28	0	Yes
Pyrodysinoic acid (**6**)	289.37	3	1	2.43	0	Yes
Avinosol (**7**)	564.67	8	4	2.28	1	Yes
Puupehenone (**8**)	328.45	3	1	2.98	0	Yes
α-Santonin (**9**)	246.30	3	0	2.38	0	Yes
4'-Methylaminoavarone (**10**)	341.49	3	2	3.11	0	Yes
3'-Methylaminoavarone (**11**)	341.49	2	1	3.11	0	Yes
Diplopuupehenone (**12**)	659.89	6	3	5.03	2	No
Dysideanin B (**13**)	242.30	1	2	1.65	0	Yes

Discussion

Secondary metabolites are small organic compounds produced by organisms to help them adapt to environmental pressures, despite not being essential to primary metabolism [37-39]. Marine sessile organisms, particularly sponges, are prolific sources of such compounds due to their constant exposure to intense biotic and abiotic stressors in competitive ecosystems [40]. Among marine organisms, sponges have attracted considerable interest for their chemically diverse secondary metabolites with demonstrated pharmaceutical properties, including antimicrobial, antifungal, and antiviral activities [41-43].

Thirteen *Dysidea* metabolites were reported in our results for their favorable *in silico* inhibitory activities against protein tyrosine phosphatase 1B (PTP1B), a validated target in metabolic disease (e.g., type 2 diabetes) and cancer therapy. Several of these, such as avarol (**1**), avarone (**2**), α-santonin (**9**), 4′-methylaminoavarone (**10**), and 3′-methylaminoavarone (**11**), are sesquiterpenes from *D. avara* [24]. Looking into their structures and previously reported bioactivities, avarol (**1**) and its oxidized derivative avarone (**2**) possess a bicyclic sesquiterpene moiety that may contribute to multifunctional PTP1B inhibition [44]. α-Santonin (**9**) is noted for anti-inflammatory, antioxidant, immunosuppressive, and anticancer properties [45]. The methylaminoavarone derivatives **10** and **11** show cytotoxicity and protein kinase inhibition [46]. Nakafuran 8 (**4**), from *D. fragilis*, features a rare bicyclodecadiene-furan skeleton with a bridgehead quaternary carbon, contributing to its potent PTP1B activity [47]. Haterumadysin A (**5**), isolated from *D. chlorea*, has a spirofused furan-bicyclononane structure and a rare spirolactol moiety, known for disrupting cell division [48]. Furodysin (**3**) and pyrodysinoic acid (**6**), from *Dysidea* and *D. robusta*, respectively, are sesquiterpenes with unique carbocyclic or amino acid-fused furan structures, valuable as synthetic scaffolds for drug development [49-50]. Avinosol (**7**), a meroterpenoid-nucleoside conjugate, displays anti-invasion activity and is the first of its kind discovered in nature [51-52]. Puupehenone (**8**), a tetracyclic drimane-type sesquiterpene, stands out due to its broad biological activities, including cytotoxicity, angiogenesis inhibition, and antimicrobial effects, attributed to its quinone-methide moiety.

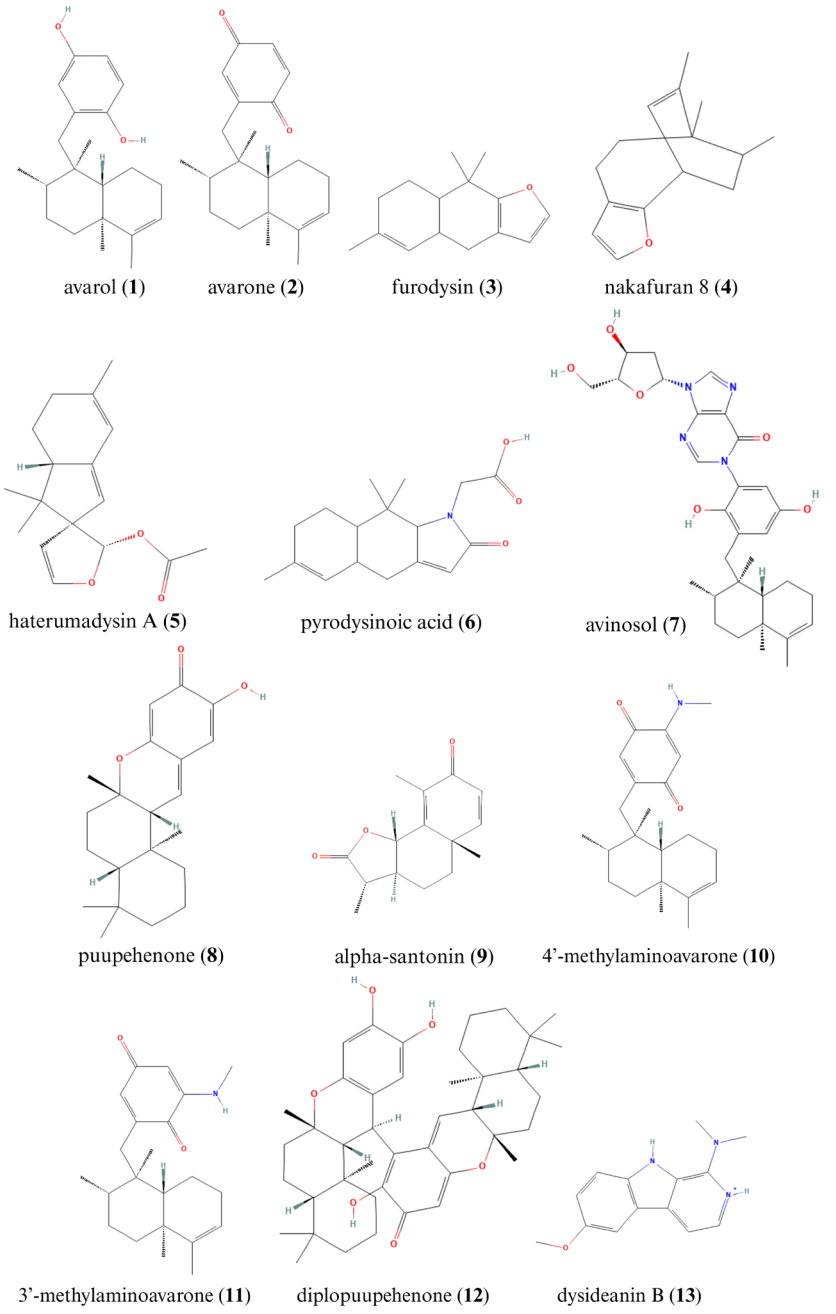

Figure 1. PubChem structures of the top thirteen compounds from the genus *Dysidea* with the highest affinity (BE > 7.0 kcal/mol) for PTP1B.

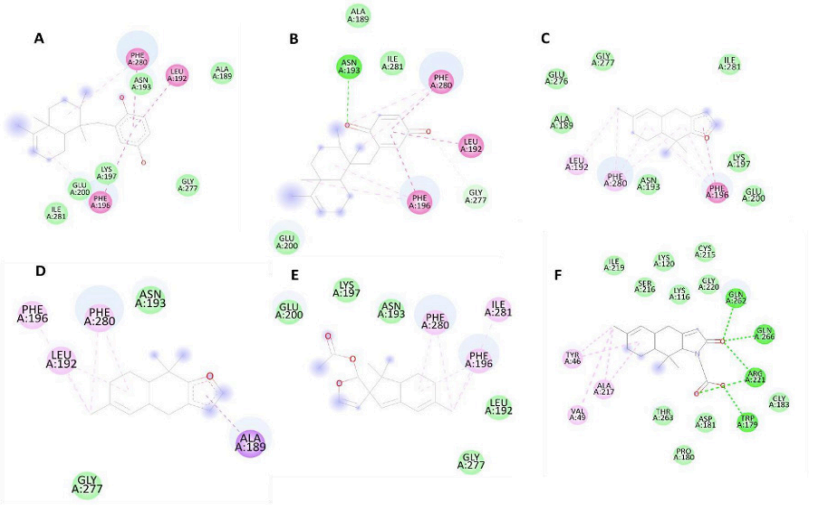

Figure 2. 2D diagram of interactions formed between the top six-binding compounds and residues at the allosteric binding site of PTP1B: Avarol (**A**), Avarone (**B**), Furodysin (**C**), Nakafuran 8 (**D**), Haterumadysin A (**E**) & Pyrodysinoic acid (**F**).

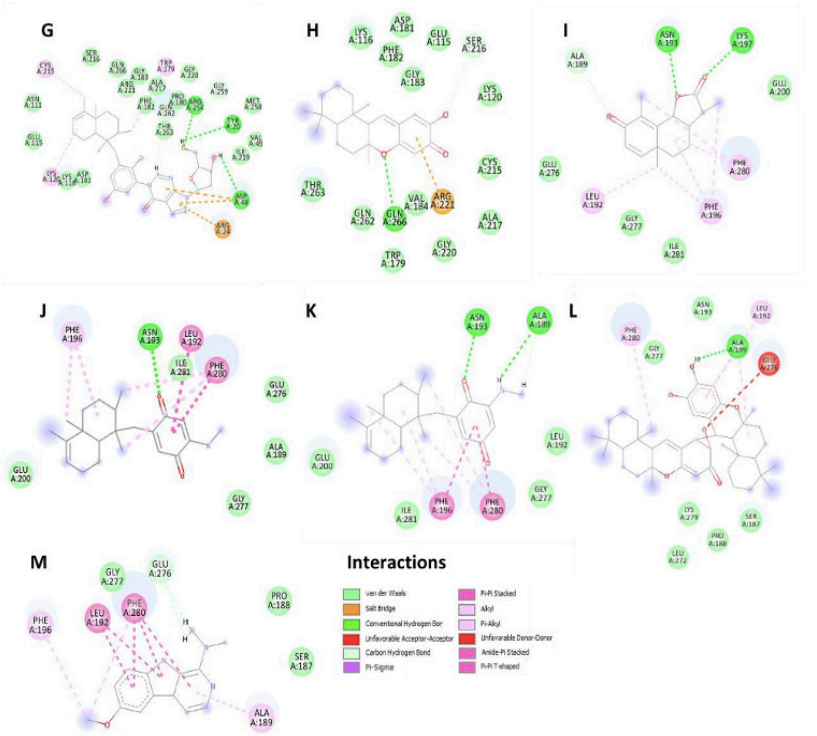

Figure 3. 2D diagram of interactions formed between the remaining seven top-binding compounds and residues at the allosteric binding site of PTP1B: Avinosol (**G**), Puupehenone (**H**), α-santonin (**I**), 4'-Methylminoavarone (**J**), 3'-Methylminoavarone (**K**), Diplopuupehenone (**L**) & Dysideanin B (**M**).

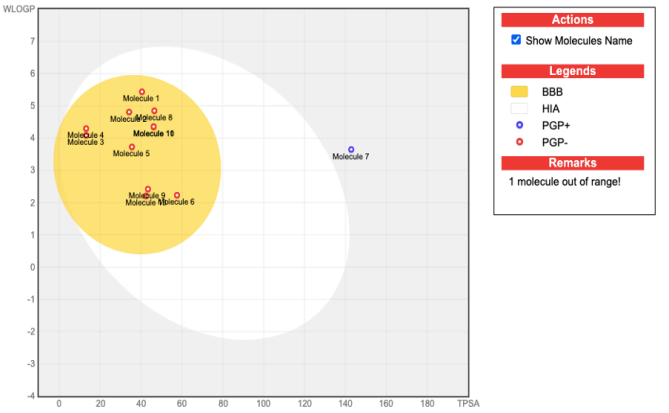

Figure 4. BOILED-Egg predictions showing gastrointestinal absorption and blood-brain barrier permeability of the top 13 compounds.

Its dimeric form, diplopuupehenone (**12**), retains similar bioactivities [53-54]. Lastly, dysideanin B (**13**), an indole alkaloid from *Dysidea*, shows antibacterial and moderate PTP1B inhibition [55]. The chemical and biological diversity exhibited by these secondary metabolites, particularly regarding PTP1B inhibition, highlights their potential as lead compounds for therapeutic development.

Enzymes have active sites for substrate binding and allosteric sites that regulate their activity. PTP1B, a diabetes target, has a highly conserved active site centered on Cysteine 215, making selective inhibition difficult due to its similarity to other PTPs like TCPTP [5]. Active-site inhibitors also face challenges penetrating cells as they mimic negatively charged phosphotyrosine residues. Consequently, drug development has shifted toward the more hydrophobic, less conserved allosteric site, enabling safer and more selective inhibition, exemplified by lupane triterpenes [56-57]. X-ray studies locate the allosteric site about 20 Å from the catalytic site, near the WPD loop (Trp179, Pro180, Asp181), which shifts between an "open" (substrate accessible) and "closed" (catalytically active) state. Allosteric inhibitors lock this loop open, blocking catalysis [6]. Molecular docking on PTP1B's allosteric site (PDB ID: 1T49) highlights key residues such as Asn193, Phe196, and Phe280. Compounds like α-santonin and methylaminoavarones bind mainly via π-π stacking, stabilized by van der Waals forces that may hinder loop movement. These interactions potentially disrupt the hydrogen bond network within the α3-α6-α7 helices, which is essential for WPD loop closure and thus PTP1B activation [6, 58-61]. In our docking, all compounds were analyzed within a 22.5 Å cube to identify binding poses, confirming these critical interactions and supporting their potential as allosteric inhibitors that prevent the WPD loop from closing and enabling catalysis.

Key residues within the hydrophobic pocket of PTP1B's allosteric site, specifically LEU192, PHE196, and PHE280, are crucial for inhibitory activity (Shrestha et al., 2019). All compounds tested in our study, except puupehenone (**8**), avinosol (**7**), and pyrodysinoic acid (**6**), interacted with PHE196 and PHE280. Notably, avarol (**1**), avarone (**2**), and dysideanin B (**13**) interacted with all three residues (LEU192, PHE196, and PHE280), highlighting their strong inhibitory potential. Additional residues such as ASN193 and GLU276 are also involved in hydrophobic interactions at the allosteric site. Diplopuupehenone (**12**) showed binding with PHE280 and GLU276, further supporting its potential as an effective allosteric inhibitor.

Conclusion

This study demonstrated that thirteen secondary metabolites from marine sponges of the genus *Dysidea* exhibit strong binding affinity toward the allosteric site of PTP1B, a key enzyme implicated in type 2 diabetes (T2D). Molecular docking of thirty-one distinct compounds revealed these thirteen as potential PTP1B inhibitors with favorable docking scores. Eleven of the thirteen *Dysidea* secondary metabolites have favorable drug-likeness and pharmacokinetic profiles *in silico*. The findings underscore the value of targeting the allosteric site of PTP1B to achieve both potency and selectivity in drug design. These results support further laboratory validation of the identified compounds as promising therapeutic candidates for T2D. Additionally, the molecular docking data provide a valuable foundation for prioritizing drug candidates prior to experimental testing.

Acknowledgments

The authors thank the Department of Biological Sciences, College of Science, University of Santo Tomas, for the support and guidance to the researchers.

Conflict of Interest

The authors declare no conflict of interest.

Author Contributions

Conceptualization, GAJL, MNCA, AJADJ, GGMG, VJMJ, JDAR, and IBR; methodology, GAJL, MNCA, AJADJ, GGMG, VJMJ and JAHM; data collection GAJL, MNCA, AJADJ, GGMG, VJMJ and JAHM; analysis and interpretation of data, GAJL, MNCA, AJADJ, GGMG, VJMJ, JAHM, JDAR and IBR; original draft preparation, GAJL, MNCA, AJADJ, GGMG and VJMJ; review and editing of the draft, GAJL, MNCA, AJADJ, GGMG, VJMJ, JAHM, JDAR and IBR. All authors have read and agreed to the final version of the manuscript.

Institutional Review Board Statement

Not applicable.

Informed Consent Statement

Not applicable.

References

[1] World Health Organization. Diabetes. World Health Organization 2021; November 10. Retrieved April 19, 2022 from https://www.who.int/news-room/fact-sheets/detail/diabetes.

[2] Magliano DJ, & Boyko EJ. IDF Diabetes Atlas 10th edition scientific committee. IDF Diabetes Atlas. 10th ed. International Diabetes Federation, Brussels; 2021.

[3] Tahrani A, Bailey C, Del Prato S, & Barnett A. Management of type 2 diabetes: New and future developments in treatment. Lancet 2011; 378, 182–197.

[4] Jiang CS, Liang LF, & Guo YW. Natural products possessing protein tyrosine phosphatase 1B (PTP1B) inhibitory activity found in the last decades. Acta Pharmacologica Sinica 2012; 33(10), 1217–1245.

[5] Popov D. Novel protein tyrosine phosphatase 1B inhibitors: Interaction requirements for improved intracellular efficacy in type 2 diabetes mellitus and obesity control. Biochemical and Biophysical Research Communications 2011; 410(3), 377–381.

[6] Shinde R, Kumar G, Eqbal S, & Sobhia M. Screening and identification of potential PTP1B allosteric inhibitors using in silico and in vitro approaches. Plos One 2018; 13(6), e0199020.

[7] Abdelsalam SS, Korashy HM, Zeidan A, & Agouni A. The role of protein tyrosine phosphatase (PTP)-1B in cardiovascular disease and its interplay with insulin resistance. Biomolecules 2019; 9(7), 286.

[8] Hendriks WJ, Elson A, Harroch S, Pulido R, Stoker A, & den Hertog J. Protein tyrosine phosphatases in health and disease. The FEBS Journal 2013; 280(2), 708–730.

[9] Cho H. Protein tyrosine phosphatase 1B (PTP1B) and obesity. Vitamins & Hormones 2013; 91, 405–424.

[10] Teimouri M, Hosseini H, ArabSadeghabadi Z, Babaei-Khorzoughi R, Gorgani-Firuzjaee S, & Meshkani R. The role of protein tyrosine phosphatase 1B (PTP1B) in the pathogenesis of type 2 diabetes mellitus and its complications. Journal of Physiology and Biochemistry 2022; 1–16.

[11] Ezzat SM, Bishbishy MHE, Habtemariam S, Salehi B, Sharifi-Rad M, Martins N, & Sharifi-Rad J. Looking at marine-derived bioactive molecules as upcoming anti-diabetic agents: A special emphasis on PTP1B inhibitors. Molecules 2018; 23(12), 3334.

[12] Song GJ, Jung M, Kim JH, Park H, Rahman MH, Zhang S, Zhang ZY, Park DH, Kook H, Lee IK, & Suk K. A novel role for protein tyrosine phosphatase 1B as a positive regulator of neuroinflammation. Journal of Neuroinflammation 2016; 13(1).

[13] De Caralt S, Bry D, Bontemps N, Turon X, Uriz MJ, & Banaigs B. Sources of secondary metabolite variation in Dysidea avara (Porifera: Demospongiae): The importance of having good neighbors. Marine Drugs 2013; 11(2), 489–503.

[14] Cormack S, Kelly M, & Battershill C. Description of two new species of Dysidea (Porifera, Demospongiae, Dictyoceratida, Dysideidae) from Tauranga Harbour, Bay of Plenty, New Zealand. Zootaxa 2020; 4780(3), 523–542.

[15] Ferreira LG, Dos Santos RN, Oliva G, & Andricopulo AD. Molecular docking and structure-based drug design strategies. Molecules 2015; 20(7), 13384–13421.

[16] Wang X, Song K, Li L, & Chen L. Structure-based drug design strategies and challenges. Current Topics in Medicinal Chemistry 2018; 18(12), 998–1006.

[17] Aparoy P, Reddy KK, & Reddanna P. Structure and ligand based drug design strategies in the development of novel 5-LOX inhibitors. Current Medicinal Chemistry 2012; 19(22), 3763–3778.

[18] Manzano JAH, Brogi S, Calderone V, Macabeo APG, & Austriaco N. Globospiramine exhibits inhibitory and fungicidal effects against Candida albicans via apoptotic mechanisms. Biomolecules 2024; 14(6), 610.

[19] Amandy FV, Neri GL, Manzano JA, Go AD, & Macabeo AP. Polypharmacology-driven discovery and design of highly selective, dual and multitargeting inhibitors of Mycobacterium tuberculosis—a review. Current Drug Targets 2024; 25(9), 620–634.

[20] Manzano JAH, Abellanosa EA, Aguilar JP, Brogi S, Yen CH, Macabeo APG, & Austriaco N. Globospiramine from Voacanga globosa exerts robust cytotoxic and antiproliferative activities on cancer cells by inducing caspase-dependent apoptosis in A549 cells and inhibiting MAPK14 (p38α): in vitro and computational investigations. Cells 2024; 13(9), 772.

[21] Tan MA, Manzano JAH, & Ishikawa H. Amyloid-beta aggregation and advanced glycation end-products inhibitory activities of Pandanus amaryllifolius Roxb. alkaloids: Insights from in vitro and computational investigations. Chemical Papers 2024; 1–9.

[22] Manzano JAH, Llames LCJ, & Macabeo APG. Tetrahydrobisbenzylisoquinoline alkaloids from Phaeanthus ophthalmicus inhibit target enzymes associated with type 2 diabetes and obesity. Journal of Applied Pharmaceutical Science 2024; 14(1), 230–237.

[23] Garcia KYM, Manzano JAH, & Macabeo APG. An α-glucosidase and pancreatic lipase inhibitory cytochalasan derivative from the Dothideomycetes fungus, Sparticola triseptata. Acta Manilana 2023; 71, 97–109.

[24] Chandra M. Secondary metabolites composition and geographical distribution of marine sponges of the genus Dysidea [MS Thesis]. The University of the South Pacific; 2009. Coral Reef Initiatives for the Pacific (CRISP).

[25] Siengalewicz P, Mulzer J, & Rinner U. 2.15 Selected Diastereoselective Reactions: Substrate Controlled Stereoselective Conjugate Addition Reactions with Organocopper Reagents. Comprehensive Chirality 2012; 441–471.

[26] De Caralt S, Bry D, Bontemps N, Turon X, Uriz MJ, & Banaigs B. Sources of secondary metabolite variation in Dysidea avara (Porifera: Demospongiae): The importance of having good neighbors. Marine Drugs 2013; 11(2), 489–503.

[27] Van Kiem P, Nhiem NX, Tai BH, Anh HLT, Hang DTT, Cuc NT, Huyen LT, Nam NH, Yen PH, Thung DC, & Van Minh C. Bis-sesquiterpene from the marine sponge Dysidea fragilis. Natural Product Communications 2016; 11(4), 1934578X1601100.

[28] Ramage KS, Taki AC, Lum KY, Hayes S, Byrne JJ, Wang T, Hofmann A, Ekins MG, White JM, Jabbar A, Davis RA, & Gasser RB. Dysidenin from the marine sponge Citronia sp. affects the motility and morphology of Haemonchus contortus larvae in vitro. Marine Drugs 2021; 19(12), 698.

[29] Romano G, Almeida M, Varela Coelho A, Cutignano A, Gonçalves LG, Hansen E, Khnykin D, Mass T, Ramšak A, Rocha MS, Silva TH, Sugni M, Ballarin L, & Genevière A-M. Biomaterials and bioactive natural products from marine invertebrates: From basic research to innovative applications. Marine Drugs 2022; 20(4), 219.

[30] National Center for Biotechnology Information. PubChem Compound Summary for CID 128257, Dysidenine. 2022. Retrieved April 16, 2022 from https://pubchem.ncbi.nlm.nih.gov/compound/Dysidenine.

[31] Ibana FV, de Leon VNO, Manzano JAH, Castillo AL, & Macabeo APG. Alkenylated phenolics from Syzygium lineatum with antiproliferative activity against chronic myeloid leukemia cells. Journal of Applied Pharmaceutical Science 2024; 14(08), 070–077.

[32] Pettersen EF, Goddard TD, Huang CC, Couch GS, Greenblatt DM, Meng EC, & Ferrin TE. UCSF Chimera—a visualization system for exploratory research and analysis. Journal of Computational Chemistry 2004; 25(13), 1605–1612.

[33] Garcia KYM, Manzano JAH, & Macabeo APG. An α-glucosidase and pancreatic lipase inhibitory cytochalasan derivative from the Dothideomycetes fungus, Sparficola triseptata. Acta Manilana 2023; 71, 97–109.

[34] Eberhardt J, Santos-Martins D, Tillack AF, & Forli S. AutoDock Vina 1.2.0: New docking methods, expanded force field, and Python bindings. Journal of Chemical Information and Modeling 2021.

[35] Manzano JAH, Cruz C, Quimque MTJ, & Macabeo APG. In silico potentials of Alpinia galanga constituents against human placental aromatase vital in postmenopausal estrogen-dependent breast cancer pathogenesis. Philippine Journal of Science 2022; 151, 2101–2115.

[36] Daina A, & Zoete V. A boiled□egg to predict gastrointestinal absorption and brain penetration of small molecules. ChemMedChem 2016; 11(11), 1117–1121.

[37] Monfil VO, & Casas-Flores S. Molecular mechanisms of biocontrol in Trichoderma spp. and their applications in agriculture. Biotechnology and Biology of Trichoderma 2014; 429–453.

[38] Mosunova O, Navarro-Muñoz JC, & Collemare J. The biosynthesis of fungal secondary metabolites: From fundamentals to biotechnological applications. Encyclopedia of Mycology 2021; 458–476.

[39] Srivastava P, Singh M, & Chaturvedi R. Herbal medicine and biotechnology for the benefit of human health. Animal Biotechnology 2020; 613–629.

[40] Conte M, Fontana E, Nebbioso A, & Altucci L. Marine-derived secondary metabolites as promising epigenetic bio-compounds for anticancer therapy. Marine Drugs 2020; 19(1), 15.

[41] Petersen LE, Kellermann MY, & Schupp PJ. Secondary metabolites of marine microbes: From natural products chemistry to chemical ecology. In: Jungblut S, Liebich V, Bode-Dalby M, editors. The Oceans: Our Research, Our Future. Springer, Cham; 2020.

[42] Hussein RA, & El-Anssary AA. Plants secondary metabolites: The key drivers of the pharmacological actions of medicinal plants. In: Herbal Medicine. IntechOpen; 2018.

[43] Seca A, & Pinto D. Biological potential and medical use of secondary metabolites. Medicines 2019; 6(2), 66.

[44] Abdjul DB, Yamazaki H, Takahashi O, Kirikoshi R, Ukai K, & Namikoshi M. Sesquiterpene hydroquinones with protein tyrosine phosphatase 1B inhibitory activities from a Dysidea sp. marine sponge collected in Okinawa. Journal of Natural Products 2016; 79(7), 1842–1847.

[45] Aghvami M, Keshavarz A, Nazemi M, Zarei MH, & Pourahmad J. Selective cytotoxicity of α-santonin from the Persian Gulf sponge Dysidea avara on pediatric ALL B-lymphocytes via mitochondrial targeting. Asian Pacific Journal of Cancer Prevention 2018; 19(8), 2149–2154.

[46] Hamed ANES, Wätjen W, Schmitz R, Chovolou Y, Edrada-Ebel R, Youssef DT, ... & Proksch P. A new bioactive sesquiterpenoid quinone from the Mediterranean Sea marine sponge Dysidea avara. Natural Product Communications 2013; 8(3), 289-292.

[47] Hou BL, Wong JJ, Lv N, Wang YQ, Houk KN, & Li CC. Facile generation of bridged medium-sized polycyclic systems by rhodium-catalysed intramolecular (3+2) dipolar cycloadditions. Nature Communications 2021; 12(1).

[48] Blunt JW, Copp BR, Hu WP, Munro MHG, Northcote PT, & Prinsep MR. Marine natural products. Natural Product Reports 2012; 25(1), 35.

[49] Berlinck RGS, Crnkovic CM, Gubiani JR, Bernardi DI, Ióca LP, & Quintana- Bulla JI. The isolation of water-soluble natural products – challenges, strategies and perspectives. Natural Product Reports 2022; 39(3), 596–669.

[50] Baharfar R, Asghari S, & Peiman S. Synthesis of novel rhodanine based functionalized furans from the reaction of tert-butyl isocyanide with acetylenic esters in the presence of rhodanine acetic acid derivatives. Arabian Journal of Chemistry 2019; 12(7), 1496–1500.

[51] Han J, Jiang L, Zhang L, Quinn RJ, Liu X, & Feng Y. Peculiarities of meroterpenoids and their bioproduction. Applied Microbiology and Biotechnology 2021; 105(10), 3987–4003.

[52] Russo D & Milella L. Analysis of meroterpenoids. In: Recent advances in natural products analysis, pp. 477–501. Elsevier; 2020.

[53] Menna M, Imperatore C, D'Aniello F, & Aiello A. Meroterpenes from Marine Invertebrates: Structures, Occurrence, and Ecological Implications. Marine Drugs 2013; 11(5), 1602–1643.

[54] Ebrahim H & el Sayed K. Discovery of Novel Antiangiogenic Marine Natural Product Scaffolds. Marine Drugs 2016; 14(3), 57.

[55] Netz N & Opatz T. Marine Indole Alkaloids. Marine Drugs 2015; 13(8), 4814–4914.

[56] Wenthur CJ, Gentry PR, Mathews TP, & Lindsley CW. Drugs for Allosteric Sites on Receptors. Annual Review of Pharmacology and Toxicology 2014; 54(1), 165–184.

[57] Jin T, Yu H, & Huang XF. Selective binding modes and allosteric inhibitory effects of lupane triterpenes on protein tyrosine phosphatase 1B. Scientific Reports 2016; 6(1).

[58] Li S, Zhang J, Lu S, Huang W, Geng L, Shen Q, & Zhang J. The Mechanism of Allosteric Inhibition of Protein Tyrosine Phosphatase 1B. PLoS ONE 2014; 9(5), e97668.

[59] Peng H, Li Q, & Chen T. Industrial applications of carbon nanotubes. Elsevier; 2017.

[60] Baskaran SK, Goswami N, Selvaraj S, Muthusamy VS, & Lakshmi BS. Molecular Dynamics Approach to Probe the Allosteric Inhibition of PTP1B by Chlorogenic and Cichoric Acid. Journal of Chemical Information and Modeling 2012; 52(8), 2004–2012.

[61] Agoni C, Ramharack P, & Soliman MES. Allosteric inhibition induces an open WPD-loop: a new avenue towards glioblastoma therapy. RSC Advances 2018; 8(70), 40187–40197.

Supplementary Table 1. The binding energy scores of the thirty-one compounds previously isolated from the screened marine sponge genus *Dysidea* for molecular docking.

Compound	Binding energy values (kcal/mol)
Dysidine	-6.7
Avarol	-7.4
Dysidotronic acid	-6.6
Arenarol	-6.8
Avarone	-7.4
Dysidenone A	-5.8
Furodysin	-7.6
Nakafuran 8	-7.1
Nakafuran 9	-6.3
Haterumadysin A	-7.3
Haterumadysin C	-4.8
Haterumadysin D	-5.1
Pyrodysinoic acid	-7.6
Bolinaquinone	-6.6
7-deacetoxyolepupuane	-6.7
Avinosol	-7.8
Dysidiolide	-6.8
Dendrolasin	-6.6
Puupehenone	-7.0
Dehydroherbadysidolide	-6.2
α-Santonin	-7.4
4'-Methylaminoavarone	-7.4
3'-methylaminoavarone	-7.6
Dysidamide D	-6.4
Dicynone	-2.9
Diplopuupehenone	-7.9
Isodysidenin	-6.1
Dysithiazolamide	-6.4
Dysideasterol F	-6.9
Dysideanin A	-3.9
Dysideanin B	-7.0